

## Magnesium Complexes

## Ring-Shaped Phosphinoamido-Magnesium-Hydride Complexes: Syntheses, Structures, Reactivity, and Catalysis

Lea Fohlmeister<sup>[a]</sup> and Andreas Stasch<sup>\*[a, b]</sup>*Dedicated to Professor Herbert W. Roesky on the occasion of his 80th birthday*

**Abstract:** A series of magnesium(II) complexes bearing the sterically demanding phosphinoamide ligand,  $L^- = Ph_2PNDip^-$ ,  $Dip = 2,6$ -diisopropylphenyl, including heteroleptic magnesium alkyl and hydride complexes are described. The ligand geometry enforces various novel ring and cluster geometries for the heteroleptic compounds. We have studied the stoichiometric reactivity of  $[(LMgH)_4]$  towards unsaturated substrates, and investigated catalytic hydroborations

and hydrosilylations of ketones and pyridines. We found that hydroborations of two ketones with pinacolborane using various Mg precatalysts is very rapid at room temperature with very low catalyst loadings, and ketone hydrosilylation using phenylsilane is rapid at 70 °C. Our studies point to an insertion/ $\sigma$ -bond metathesis catalytic cycle of an in situ formed "MgH<sub>2</sub>" active species.

## Introduction

Metal hydrides and their complexes play a fundamental role in many applications including as hydride sources in synthesis and catalysis, and for hydrogen storage technologies.<sup>[1]</sup> Of the binary hydrogen compounds of the chemical elements, *s*-block metal hydrides are unique due to the highly electropositive nature of the alkali and alkaline earth metals, and their electronegativity difference from hydrogen. Thus, these metal hydrides are generally classified as ionic or saline.<sup>[2,3]</sup> Furthermore, the *s*-block is home to highly earth-abundant, non-toxic and even biocompatible metals such as Na, K, Mg and Ca, all of which offer a range of properties for future sustainable chemical applications.<sup>[4]</sup> A range of well-defined *s*-block metal-hydride complexes have been reported in very recent years, and these have already been successfully used in stoichiometric and catalytic transformations. In addition, the hydrogen storage properties of some of these examples have been investigated.<sup>[2,3]</sup> The recent success in this area can be attributed to both the development of suitable synthetic strategies to generate *s*-block metal-hydride fragments, and the design and use of stabilising ligand systems that prevent dismutation and other decomposition reactions of the formed complexes, leading to the precipitation of insoluble saline metal hydrides. Gen-

erally, the ionic and flexible metal-ligand interactions in *s*-block metal coordination chemistry require ligand systems that suppress dismutation equilibria, such as chelating, bridging, and/or sterically demanding ligands.<sup>[2,3]</sup>

The majority of well-defined *s*-block metal hydride complexes has been prepared with magnesium, and these encompass complexes with sterically demanding  $\beta$ -diketiminates,<sup>[5]</sup> mixed *s*-block amido species,<sup>[6]</sup> and a variety of other carbon-, nitrogen- or oxygen-based ligand species,<sup>[7,8]</sup> as well as a few examples of related calcium hydride complexes.<sup>[9]</sup> They have been accessed through either hydride metathesis using magnesium alkyl or amido fragments with main group element hydride species (such as silanes, boranes or alanes),  $\beta$ -hydrogen elimination, or hydrogenation of dimeric magnesium(I) compounds with cyclohexadiene or alane complexes. The newly formed complexes show both interesting stoichiometric and catalytic reactivity.<sup>[2,10-13]</sup> For several catalytic applications, the active magnesium hydride catalyst was conveniently generated in situ from stoichiometric hydride sources such as boranes and silanes.<sup>[2,10,11]</sup>

We have previously employed the simple, sterically demanding phosphinoamide ligand  $Ph_2PNDip^-$  ( $Dip = 2,6$ -diisopropylphenyl), (designated as  $L^-$ ), to obtain the well-defined and hydrocarbon-soluble lithium hydride complex  $[(LL)_4(LiH)_4]$ , as well as studied its properties and reactivity.<sup>[14]</sup> Here we report the extension to magnesium hydride complexes with this ligand. We reasoned that the orientation of the donor atoms of the phosphinoamide ligand,<sup>[14,15]</sup> which typically favours bridging-coordination modes, is similar to what we found for pyrazolate ligands,<sup>[16]</sup> and could favour the formation of unprecedented cluster or ring complexes that potentially liberate reactive LMgH fragments for unusual stoichiometric and catalytic reactivity. In addition, the inclusion of the NMR-active phosphorus

[a] Dr. L. Fohlmeister, Dr. A. Stasch  
School of Chemistry, Monash University  
17 Rainforest Walk, Melbourne, Victoria 3800 (Australia)

[b] Dr. A. Stasch  
School of Chemistry, University of St Andrews  
North Haugh, St. Andrews, KY16 9ST (UK)  
E-mail: as411@st-andrews.ac.uk

Supporting information for this article can be found under  
<http://dx.doi.org/10.1002/chem.201601623>.

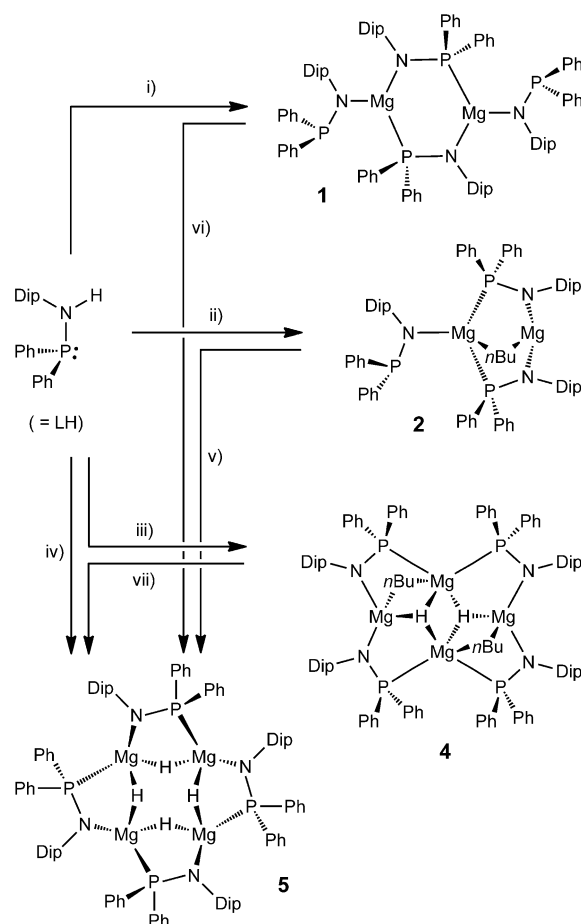
centre in the ligand system should allow for further insights into the reactivity of the newly formed compounds.

## Results and Discussion

### Synthesis

To access suitable precursor molecules to phosphinoamido-magnesium-hydride complexes, we studied the reaction of the sterically demanding phosphinoamine<sup>[15]</sup> DipNHPPH<sub>2</sub> (LH)<sup>[14b]</sup> with commercially available di-*n*-butylmagnesium in hydrocarbon solvents. The reaction of LH with Mg(*n*Bu)<sub>2</sub> in a 2:1 molar ratio afforded one main product according to <sup>1</sup>H and <sup>31</sup>P{<sup>1</sup>H} NMR spectroscopic studies. A good yield of the new complex **1** [(L<sub>2</sub>Mg)<sub>2</sub>] was isolated and the molecular structure of the complex was characterised (Scheme 1 and Figure 1). In contrast, the 1:1 molar reaction of LH with Mg(*n*Bu)<sub>2</sub> afforded a product mixture with a main species showing <sup>1</sup>H NMR spectroscopic resonances that suggest one Mg-bound *n*Bu group per three phosphinoamide ligands. A doublet and a triplet in the corresponding <sup>31</sup>P{<sup>1</sup>H} NMR spectrum suggest different phosphinoamido ligand environments in a 2:1 ratio that couple with each other. Work-up of this reaction afforded the expected complex **2** [L<sub>3</sub>Mg<sub>2</sub>(*n*Bu)], in a moderate isolated yield, which could also be structurally characterised (Scheme 1 and Figure 1). From reactions with the 1:1 molar ratio, we further obtained colourless crystals of the unusual magnesium-ethyl complex **3** [{(LMgEt)<sub>2</sub>}]<sub>6</sub> (Figure 1) in very low yield in one instance. Related to this observation, previous studies have shown that commercially available Mg(*n*Bu)<sub>2</sub> can contain other organic substituents such as ethyl groups, and even significant quantities of aluminium.<sup>[17]</sup>

The homoleptic complex **1** crystallises with half of a molecule in the asymmetric unit (Scheme 1 and Figure 1). Each Mg centre is in a planar, three-coordinate environment binding to one terminal κ<sup>1</sup>-N phosphinoamide, and to one P- and one N-donor atom of two μ-κ<sup>2</sup>-P,N phosphinoamides. In 2:1.5C<sub>5</sub>H<sub>12</sub>, Mg1 and Mg2 are bridged by two phosphinoamides, with N,N'-coordination to Mg1 and P,P'-coordination to Mg2, and also a bridging *n*Bu group. Mg2 is additionally coordinated by a terminal phosphinoamide ligand. In the solid state, Mg1 shows further short contacts to hydrogen atoms of one isopropyl group (shortest contact: Mg1...H40A of ca. 2.2 Å). Complex 3·7C<sub>6</sub>H<sub>14</sub> (Figure 1) crystallised in the trigonal crystal system, and is a large-ring system formed by six (LMgEt)<sub>2</sub> subunits. In the latter, two Mg in the asymmetric unit are bridged by two phosphinoamides and one ethyl group so that each Mg atom is P,N,C-coordinated. In addition, Mg2 binds to the carbon atom of a "terminal" ethyl group that is coordinated via short Mg...H contacts to the Mg1' centre of the next Mg<sub>2</sub> subunit, forming the connective backbone of the (Mg...Mg-CH<sub>2</sub>...)<sub>6</sub> ring system. It seems that the larger butyl group does not support a stable compound in the desired 1:1 phosphinoamide:butyl stoichiometry, and thus forms **2** instead, but the smaller ethyl group in **3** does allow this composition. Furthermore, compounds **1–3** show that the preferred coordination mode of phosphinoamide ligands between two Mg centres under the



**Scheme 1.** Synthesis of complexes **1**, **2**, **4** and **5**. i) 0.5 Mg(*n*Bu)<sub>2</sub>, toluene, RT; ii) Mg(*n*Bu)<sub>2</sub>, toluene, RT; iii) Mg(*n*Bu)<sub>2</sub>, PhSiH<sub>3</sub>, *n*-hexane, 60 °C; iv) Mg(*n*Bu)<sub>2</sub>, PhSiH<sub>3</sub>, toluene, 70 °C; v), vi) and vii) PhSiH<sub>3</sub>, 60–70 °C, benzene or toluene.

given conditions (e.g., non-coordinating solvents) is a *cis*-like μ-κ<sup>2</sup>-P,N coordination bridge, though terminal κ<sup>1</sup>-N-coordination is observed as well.

In deuterated benzene solution, the homoleptic complex **1** only shows one doublet and one septet for the protons of the isopropyl groups in its <sup>1</sup>H NMR spectrum, and one singlet in its <sup>31</sup>P{<sup>1</sup>H} NMR spectrum (56.4 ppm). This symmetry is supportive of fast ligand exchange processes under these conditions, which can be expected for highly fluxional s-block metal ion–ligand interactions. In deuterated THF, the compound shows two broad methyl and one broad methine resonances at room temperature that resolve to one broad methyl resonance and a sharp methine septet at 60 °C, respectively, in the <sup>1</sup>H NMR spectra (Figures S2 and S3, Supporting Information). Complex **2** shows broadened and overlapping resonances for the isopropyl groups in its <sup>1</sup>H NMR spectrum recorded in deuterated benzene, and a doublet (δ = 29.8 ppm) and triplet (δ = 42.7 ppm) in its <sup>31</sup>P{<sup>1</sup>H} NMR spectrum with a <sup>2</sup>J<sub>P–P</sub> coupling of 30.8 Hz. This supports the retention of the overall solid-state connectivity of **2** in solution, with two different phosphinoamide ligands in a ratio of 2:1.

Because no stable [(LMg(*n*Bu))<sub>n</sub>] complex was formed as a precursor to desired [(LMgH)<sub>n</sub>] complexes, we treated 1:1

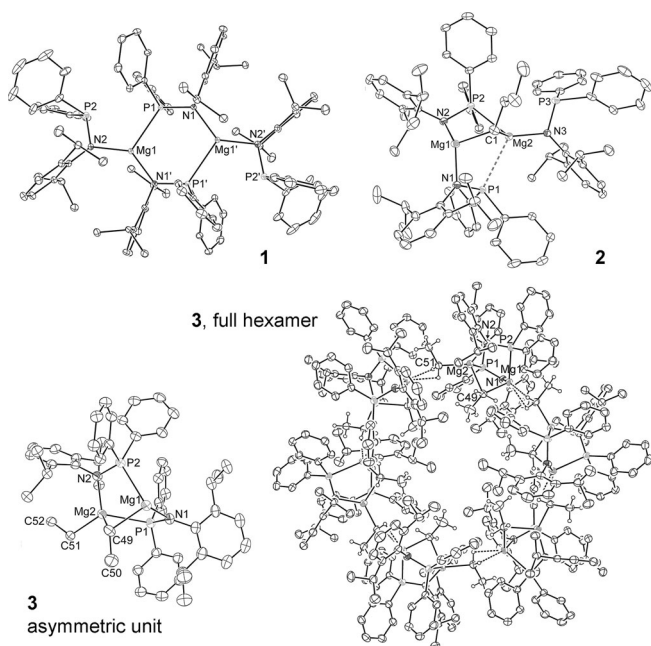


**Figure 1.** Molecular structures of **1–3** (30% thermal ellipsoids). Lattice solvent molecules and hydrogen atoms omitted, except ethyl hydrogens on full molecule **3**. Selected bond lengths [Å] and angles [°]: **1**: P(1)–N(1) 1.6770(12), P(2)–N(2) 1.6904(13), P(1)–Mg(1) 2.6318(7), P(2)–Mg(1) 2.9212(7), N(1)–Mg(1) 2.0008(12); N(2)–Mg(1)–N(1) 132.48(5), N(2)–Mg(1)–P(1) 117.77(4), N(1)–Mg(1)–P(1) 109.68(4). **2**: P(1)–N(1) 1.6618(12), P(2)–N(2) 1.6731(11), P(3)–N(3) 1.6920(12), P(1)–Mg(2) 2.9492(11), P(2)–Mg(2) 2.6910(8), P(3)–Mg(2) 3.0095(10), Mg(2)–N(3) 1.9829(12), Mg(1)–N(1) 1.9938(12), Mg(1)–N(2) 2.0191(12), Mg(1)–C(1) 2.2446(17), Mg(2)–C(1) 2.2583(16); N(3)–Mg(2)–C(1) 122.81(6), N(3)–Mg(2)–P(2) 121.81(4), C(1)–Mg(2)–P(2) 94.77(5), N(3)–Mg(2)–P(1) 120.69(4), C(1)–Mg(2)–P(1) 87.90(5), P(2)–Mg(2)–P(1) 101.30(3), N(1)–Mg(1)–N(2) 125.51(6), N(1)–Mg(1)–C(1) 104.52(6), N(2)–Mg(1)–C(1) 117.26(5). **3**: P(1)–N(1) 1.668(3), P(2)–N(2) 1.648(3), P(1)–Mg(2) 2.7971(15), Mg(1)–P(2) 2.6786(14), Mg(1)–N(1) 2.030(3), Mg(2)–N(2) 2.044(3), Mg(1)–C(49) 2.277(3), Mg(2)–C(49) 2.290(3), Mg(2)–C(51) 2.203(3), C(51)–Mg(1) 2.400(3); N(1)–Mg(1)–P(2) 113.77(9), N(2)–Mg(2)–C(51) 117.89(12), N(2)–Mg(2)–P(1) 108.61(9), C(51)–Mg(2)–P(1) 121.79(10), Mg(1)–C(49)–Mg(2) 82.07(10).

mixtures of LH and  $\text{Mg}(n\text{Bu})_2$  in *n*-hexane/heptane with phenylsilane under reflux or at 60 °C for 16 h. These experiments afforded the structurally characterised mixed-alkyl-hydride complex **4** [ $\text{L}_2\text{Mg}_2(n\text{Bu})\text{H}$ ]<sub>2</sub> in good isolated yield, (Scheme 1 and Figure 2). In contrast, heating a 1:1 mixture of LH and  $\text{Mg}(n\text{Bu})_2$  in toluene or deuterated benzene with phenylsilane at 70 °C for 16 h afforded the tetrameric magnesium-hydride complex **5** [ $\text{LMgH}$ ]<sub>4</sub> (Scheme 1 and Figure 2). Solution NMR studies show an almost quantitative conversion to **5**, and larger scale experiments afforded the isolated complex in moderate to good yields. In addition, the hexameric complex **6** [ $\text{LMgH}$ ]<sub>6</sub> could be structurally characterised from benzene in one case as a low yield byproduct (Figure 2). Similarly, related experiments with more than one molar equivalent of  $\text{Mg}(n\text{Bu})_2$  per LH in various stoichiometries, followed by phenylsilane treatment at elevated temperatures, also yielded **5** as the main product, as judged by NMR spectroscopy and lower isolated yields of **5** in these studies. Furthermore, isolated complex **4** can be converted to **5** with phenylsilane at 70 °C in benzene or toluene for 16 h in good yield, producing the expected silane

$\text{PhSiH}_2(n\text{Bu})$  as a byproduct. We conducted similar experiments of isolated **2** with phenylsilane at 70 °C for 16 h, and found that **5** was also generated alongside  $\text{PhSiH}_2(n\text{Bu})$  as well as a new Si- and P-containing compound,  $\text{PhSiH}_2(\text{L})$  (**7**), as judged by multinuclear NMR spectroscopy.<sup>[18]</sup> We then investigated the same reaction of phenylsilane with isolated **1** at 70 °C in deuterated benzene, and found that significant quantities of **5** along with **7** were formed. After 30 h at 70 °C, the reaction mixture showed only **7** and **5** in a ratio of ca. 5:1. This observation is further evidence that magnesium-hydride species can be generated from simple homoleptic magnesium(II) complexes and main-group-hydride sources, that can be responsible for stoichiometric or catalytic reactivity of these systems.

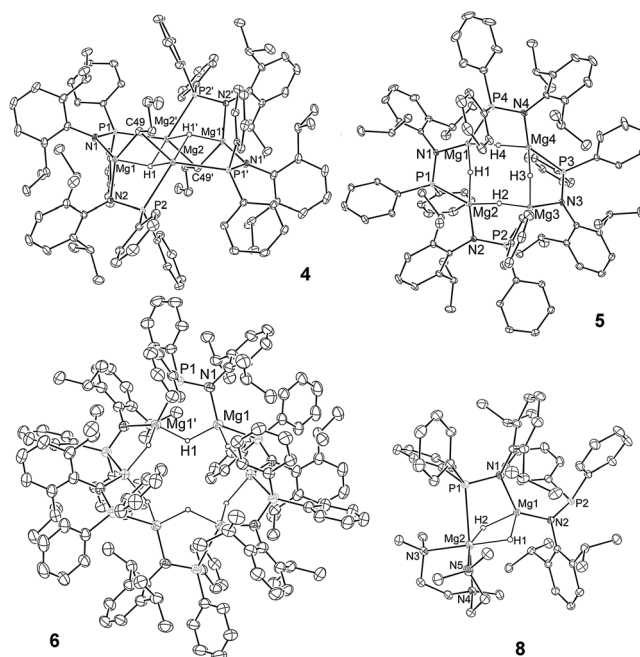


**Figure 2.** Molecular structures of magnesium-hydride species **4–6** and **8** (30% thermal ellipsoids). Lattice solvent molecules and hydrogen atoms omitted, except hydride ligands. Selected bond lengths [Å] and angles [°]: **4**: P(1)–N(1) 1.6621(13), P(2)–N(2) 1.6630(12), P(1)–Mg(2) 2.6609(7), P(1)–Mg(1) 3.0509(8), Mg(1)–P(2) 2.9555(7), P(2)–Mg(2) 2.6841(9), Mg(2)–P(1) 2.6609(7), Mg(1)–N(1) 2.0155(13), Mg(1)–N(2) 2.0275(13), Mg(1)–C(49) 2.2668(17), Mg(2)–C(49) 2.2500(16), Mg(2)–C(50) 2.7718(19), Mg(1)–H(1) 1.96(2), Mg(2)–H(1) 1.98(2), Mg(2)–H(1) 1.92(2); N(1)–Mg(1)–N(2) 132.79(5), N(1)–Mg(1)–C(49) 112.74(6), N(2)–Mg(1)–C(49) 111.70(6), N(1)–Mg(1)–H(1) 99.8(6), N(2)–Mg(1)–H(1) 95.8(6), C(49)–Mg(1)–H(1) 89.4(6), P(1)–Mg(2)–P(2) 110.18(2), C(49)–Mg(2)–H(1) 89.3(6), P(1)–Mg(2)–H(1) 133.4(6), P(2)–Mg(2)–H(1) 79.5(6). **5**: P(1)–N(1) 1.6532(11), P(2)–N(2) 1.6507(10), P(3)–N(3) 1.6458(12), P(4)–N(4) 1.6529(11), P(1)–Mg(2) 2.6074(10), Mg(1)–P(4) 2.6094(9), P(2)–Mg(3) 2.6137(8), P(3)–Mg(4) 2.6422(9), Mg(1)–N(1) 2.0029(12), Mg(2)–N(2) 2.0117(13), Mg(3)–N(3) 2.0036(11), Mg(4)–N(4) 2.0197(12), Mg(1)–H(1) 1.770(19), Mg(1)–H(4) 1.84(2), Mg(2)–H(1) 1.825(19), Mg(2)–H(2) 1.762(19), Mg(3)–H(2) 1.842(19), Mg(3)–H(3) 1.822(19), Mg(4)–H(3) 1.811(19), Mg(4)–H(4) 1.83(2), Mg...Mg 3.02 (ave, nearest); N(1)–Mg(1)–P(4) 145.53(4), Mg–H–Mg ca. 113 (ave). **6**: P(1)–N(1) 1.6553(17), P(1)–Mg(1) 2.6351(8), Mg(1)–N(1) 2.0210(16), Mg(1)–H(1) 1.92(2), Mg(1)–H(1) 1.98(2), Mg...Mg 3.24 (nearest); N(1)–Mg(1)–P(1) 122.16(5), Mg–H–Mg ca. 113. **8**: P(1)–N(1) 1.6674(18), P(2)–N(2) 1.6713(17), P(1)–Mg(2) 2.7853(11), Mg(1)–N(2) 2.0428(18), Mg(1)–N(1) 2.0887(18), Mg(1)–H(1) 1.82(3), Mg(1)–H(2) 1.91(3), Mg(2)–H(1) 1.90(3), Mg(2)–H(2) 1.96(3), Mg(2)–N(4) 2.224(2), Mg(2)–N(3) 2.270(2), Mg(2)–N(5) 2.375(2); N(2)–Mg(1)–N(1) 134.61(7), N(4)–Mg(2)–P(1) 171.63(6), N(3)–Mg(2)–H(1) 171.7(8), Mg–H–Mg ca. 96 (ave).

The mixed-alkyl-hydride complex  $4\text{-C}_6\text{H}_{14}$  crystallised with half a molecule in the asymmetric unit (Figure 2). In **4**, the four Mg atoms are in one plane and form a parallelogram that is similar to a distorted diamond. The four sides of the parallelogram are bridged by  $\mu\text{-}\kappa^2\text{-P,N}$ -coordinated phosphinoamides with alternating N,P- and P,N-arrangement. The Mg centre (Mg1) on the acute corner of the parallelogram is  $N,N'$ -coordinated by two bridging phosphinoamides and the Mg centre (Mg2) on the obtuse corner of the parallelogram is  $P,P'$ -coordinated by two phosphinoamides. The two phosphinoamides (P1/P1') that bridge the longer edges of the parallelogram lie in the  $\text{Mg}_4$  plane, whereas the other two phosphinoamide ligands (P2/P2') are located above and below the  $\text{Mg}_4$  plane (cf. the NMR discussion). The two *n*-butyl groups sit above and below the plane directly on the two edges of the shortest parallelogram sides, which consequently have the shortest Mg1...Mg2 distances. The two hydride ligands form  $\mu^3$ -bridges over  $\text{Mg1Mg2Mg2'}$  triangles on opposite sides of the  $\text{Mg}_4$  plane that are not occupied by *n*Bu groups. The molecular structures of the hydride complexes **5** and **6** have many similar geometrical features (Figure 2). The Mg atoms for both compounds lie in one plane, forming a distorted square in **5** and a perfect hexagon in **6**. In both structures, phosphinoamide ligands bridge two Mg centres on the outside of each edge and alternately lie above or below the respective  $\text{Mg}_n$  ( $n=4$  or  $6$ ) plane. The phosphinoamides are arranged around the  $(\text{MgH})_n$  core in a symmetrical, head-to-tail-like fashion. Hydride ligands bridge between two Mg atoms, again alternate above and below the  $\text{Mg}_n$  plane, and are each opposite of bridging phosphinoamide positions. The hydride ligands in **5** sit directly above or below the edges of the distorted  $\text{Mg}_4$  square, whereas those in **6** point somewhat towards the centre of the hexagon. Complex **5** is relatively symmetric showing approximate nearest contacts of  $\text{Mg}\cdots\text{N}$  (2.0 Å),  $\text{Mg}\cdots\text{P}$  (2.6 Å),  $\text{Mg}\cdots\text{H}$  (1.8 Å), and  $\text{Mg}\cdots\text{Mg}$  (3.0 Å). The symmetric hexameric species **6** shows very similar distances compared with **5**, albeit slightly larger  $\text{Mg}\cdots\text{Mg}$  separations and longer apparent Mg–H bonds.

Dissolving crystalline **4** in deuterated benzene repeatedly lead to overlapping NMR resonances for two compounds in an approximate 1:1 ratio (Figures S10 and S11 in the Supporting Information). We assigned two broad doublets ( $\delta=28.9$  and  $32.0$  ppm,  $J_{\text{P-P}}\approx 119$  Hz) in the  $^{31}\text{P}\{^1\text{H}\}$  NMR spectrum, with additional unresolved smaller coupling and a significant roof effect, to the isomer **4A** resembling the solid-state structure with head/head and tail/tail (P,N;N,P;P,N, etc.) orientation of the phosphinoamide ligands. This isomer is the more dominant species observed immediately after dissolving crystals of **4**. The other isomer **4B** shows two sharp doublets of doublets ( $\delta=27.2$  and  $38.1$ ,  $J_{\text{P-P}}\approx 20$  and  $6$  Hz, respectively) in the  $^{31}\text{P}\{^1\text{H}\}$  NMR spectrum that we believe could result from an isomer with alternating P,N-orientation of the phosphinoamide ligands, and not a different oligomeric form of  $\text{L}_2\text{Mg}_2\text{H}(n\text{Bu})$ . A DOSY NMR experiment on this isomer mixture was not conclusive, although it did point to two molecules of similar shape or size for **4A** and **4B**. New species are formed when the mixture is allowed to stand in solution at room temperature. Heating the solution of both isomers to  $80^\circ\text{C}$  followed by cooling leads

to a mixture of compounds (see Figures S12 and S13 in the Supporting Information), including small quantities of **5**, which we could in one instance characterise crystallographically from these mixtures. The non-equivalence of two different phosphinoamide ligands in **4A** becomes apparent, when the crystal structure of **4** is examined. The two phosphinoamide ligands (P1/P1') within the  $\text{Mg}_4$  plane that bridge a larger edge of the  $\text{Mg}_4$  parallelogram are different to the other two phosphinoamide ligands (P2/P2'), which bridge the smaller rhombus edge out of the plane and are affected by *n*-butyl coordination on the opposite side of the plane. Equivalence on the NMR time scale for the two different phosphinoamide environments would mainly require migration of the bridging *n*-butyl group. The MgH units of both isomers resonate as multiplets centred around 6.07 ppm (**4A**) and 5.55 ppm (**4B**) in the  $^1\text{H}$  NMR spectrum (Figure S10), or as respective singlets in the  $^1\text{H}\{^{31}\text{P}\}$  NMR spectrum. Solution NMR spectra of **5** show four doublets and two septets for the protons of the isopropyl groups, as well as one singlet ( $\delta=25$  ppm) in its  $^{31}\text{P}\{^1\text{H}\}$  NMR spectrum, in accordance with the essentially symmetrical phosphinoamide environments in the solid-state structure. The MgH resonance is observed as a very broad doublet-like multiplet ( $J\approx 54$  Hz) that resolves to a sharp singlet at  $\delta=5.14$  ppm in its  $^1\text{H}\{^{31}\text{P}\}$  NMR spectrum (see Figures S17 and S18 in the Supporting Information). Dissolving crystalline samples of **4** and **5** in the donor solvent  $[\text{D}_8]\text{THF}$  show the formation of product mixtures with essentially the same phosphinoamide-containing compounds in different ratios (see Figures S15, S16, S21 and S22 in the Supporting Information). The  $^{31}\text{P}$  NMR spectra for both compounds show significant quantities of **1** formed in solution (a singlet at  $\delta=43.9$  to  $44.0$  ppm; compare with Figure S5), especially for the spectrum of **5** (Figure S22). A broad resonance at 2.89 ppm in the  $^1\text{H}$  NMR spectra of both **4** and **5** likely accounts for a large proportion of the MgH resonances. These observations support Schlenk-type equilibria of heteroleptic complexes such as **5** in inert donor solvents, and suggest the formation of  $[\text{MgH}_2(\text{THF})_n]$  or other hydride-rich species by implication.

Upon treatment of **5** with four equivalents of the chelating amine ligand PMDETA ( $N,N,N',N',N'$ -pentamethyldiethylenetriamine), only one PMDETA ligand is coordinated to one Mg centre in a dinuclear complex with bridging hydride ligands (Figure 2) corresponding to **8**  $[(\text{L}_2\text{MgH}_2\text{Mg}(\text{PMDETA}))]$ , isolated in good yield. Complex **8** is the main and the only isolated product from reactions of varying stoichiometry, as suggested by NMR experiments. In the molecular structure of **8**, Mg2 is six-coordinate, bound to the chelating PMDETA ligand ( $N,N,N',N',N'$ - $\kappa^3$ -bound), two hydrides, and only one P atom of one phosphinoamide ligand. Mg1 is four-coordinate connected to two *N*-bound phosphinoamides and two hydride ligands. It appears that the chelating PMDETA ligand causes the loss of the sterically demanding DipN-coordination, but retains coordination to the small and hard hydride ligands. In solution, complex **8** shows broadened resonances at room temperature. At  $65^\circ\text{C}$  only one septet for the protons of the isopropyl methine groups can be found in its  $^1\text{H}$  NMR spectrum, and one broad resonance (46.3 ppm) is present in the  $^{31}\text{P}$  NMR spectrum be-

tween 25 and 65 °C, indicating fluxional ligand behaviour. The MgH resonance is found as one broad triplet ( $J_{H-P}=7.7$  Hz) in the  $^1\text{H}$  NMR spectrum, or a singlet in the  $^1\text{H}\{^{31}\text{P}\}$  NMR spectrum at 4.09 ppm, suggesting solution-averaged interactions with two phosphinoamide ligands of the same environment.

Solution studies on **4** and **5** in  $[\text{D}_8]\text{THF}$  as well as complexation of **5** with PMDETA to yield **8** highlight some of the complexities of heteroleptic coordination compounds of both ionic metal ions and bridging ligands with several possible coordination modes. The changes in coordination upon complexation of **5** with PMDETA yielding **8** may shed light on ligand redistributions when additional donor groups are available, and may be relevant to understand substrate coordination involving donor atoms before a possible hydride transfer can take place. In complex **8**, both “[PMDETA]MgH<sub>2</sub>” and “[L<sub>2</sub>Mg]” appear to be preformed, held together by the bridging hydride ligands. Equilibria between various species, including Schlenk-like equilibria, and species with various phosphinoamide coordination modes, have to be considered. Many such species are expected to have similar energies, and can likely convert with small activation energy barriers between them. These observations are important when studying and understanding the stoichiometric and catalytic reactivity of these systems, especially with an excess of molecules that contain donor atoms.

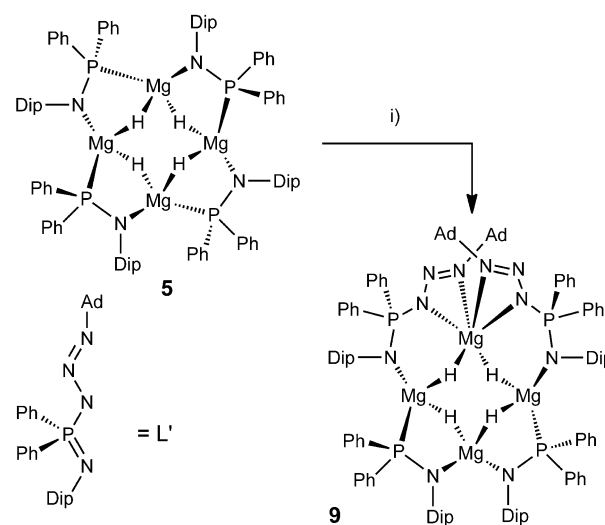
### Stoichiometric reactivity

We studied the reaction of **5** with several unsaturated organic substrates. No reaction was observed with alkenes 1,1-diphenylethene, diphenylfulvene, or diphenylacetylene in deuterated benzene.

The reaction of **5** with 1-adamantyl azide ( $\text{AdN}_3$ ) is surprisingly clean in several stoichiometric ratios as judged by in situ  $^1\text{H}$  and  $^{31}\text{P}\{^1\text{H}\}$  NMR spectroscopic studies, and the phosphazide complex **9** [ $\text{L}_2\text{L}'_2\text{Mg}_4\text{H}_4$ ] ( $\text{L}' = \text{DipNP}(\text{N}_3\text{Ad})\text{Ph}_2$ ) was obtained in low to moderate crystallised yield (Scheme 2 and Figure 3). In this complex, the hydride moieties did not react with the organic azide, as was previously found for a  $\beta$ -diketiminato-MgH system,<sup>[11f]</sup> but instead two phosphinoamide ligands were converted to anionic iminophosphorano-phosphazide ligands ( $\text{L}'^-$ ).<sup>[19,20]</sup> We have previously found that the phosphinoamide ligand ( $\text{L}^-$ ) can undergo addition reactions to several unsaturated substrates.<sup>[14a,20]</sup> The overall geometry of the  $(\text{MgH})_4^{+4}$  core in **9** is not significantly affected by this reaction compared with **5**, but the supporting ligand environment around each Mg centre has changed. This leads to three types of differently coordinated Mg centres (Figure 3). Mg1 is coordinated by two chelating  $\text{L}'^-$ -phosphazide units, whereas Mg2 and Mg4 are each coordinate by an  $\text{L}'^-$ -iminophosphorane N-atom and phosphinoamide P-atom. Consequently, Mg3 is coordinated by two phosphinoamide N-atoms. All Mg centres are still further bonded to two bridging hydride ligands. Mg1 is six-coordinate and Mg2–Mg4 are each four-coordinate. In solution, **9** shows two doublets with a small coupling constant ( $J = 2.4$  Hz) in its  $^{31}\text{P}\{^1\text{H}\}$  NMR spectrum. The resonance at 32.1 ppm is assigned to the phosphazide centre, and the one at

33.7 ppm to the phosphinoamide ligands. The chemical shifts for these resonances are surprisingly similar, considering the different phosphinoamide ( $\text{P}^{\text{III}}$ ) and iminophosphorano-phosphazide ( $\text{P}^{\text{V}}$ ) environments, which normally resonate further apart. The  $^1\text{H}$  NMR spectrum shows eight doublets and four septets for the isopropyl groups that are partially overlapping and support the retention of the overall solid-state structure in solution. The hydride ligands resonate as two multiplets, centred around  $\delta = 4.58$  and 5.16 ppm, which both couple with the  $^{31}\text{P}$  centres and each other. These couplings were demonstrated by a  $^1\text{H}-^1\text{H}$  COSY NMR spectroscopy experiment (Figure S29 in the Supporting Information), and by the fact that some coupling remains in the  $^1\text{H}\{^{31}\text{P}\}$  NMR spectrum (Figure S28). In the latter, the resonances appear as broad doublet-like multiplets ( $J \approx 8$  Hz). Similar couplings between non-equivalent MgH units of 4.5 and 5.2 Hz in magnesium hydride cluster compounds have previously been described.<sup>[5e]</sup>

Reactivity of magnesium hydride complexes towards pyridines have previously been reported, and include coordination to form a monomeric species with a terminal MgH bond,<sup>[5g]</sup> as well as several examples of pyridine hydromagnesiation products.<sup>[5c,7a,d,8b,12]</sup> The reaction of **5** with four equivalents of DMAP (4-dimethylaminopyridine) mainly led to the formation of the bis(phosphinoamido) complex  $[\text{L}_2\text{Mg}(\text{dmap})_2]$  **10** (Scheme 3), and likely MgH reaction products. Complex **10** shows expected spectroscopic features with broadened resonances for the protons of the phosphinoamido ligands, and a singlet at 44.9 ppm in its  $^{31}\text{P}\{^1\text{H}\}$  NMR spectrum. A crystal structure determination of  $\text{10} \cdot 2\text{C}_7\text{H}_8$  shows the expected connectivity and distorted tetrahedral magnesium geometry, but the data quality was too poor to be reported here (see the Supporting information for an image, Figure S54). The reaction of **5** with 12 equivalents of pyridine (Py) or DMAP cleanly led to the 1,2-hydromagnesiation products **11** [ $\text{LMg}(\text{py})_2(1,2\text{-dhp})$ ] (1,2-dhp = 1,2-dihydropyridide) and **12** [ $\text{LMg}(\text{dmap})_2(1,2\text{-dadhp})$ ] (1,2-dadhp = 4-dimethylamino-1,2-dihydropyridide), respectively (Scheme 3). The latter complex **12** was structurally



Scheme 2. Formation of complex **9** from **5**. i) 2  $\text{AdN}_3$ , benzene or toluene, RT.

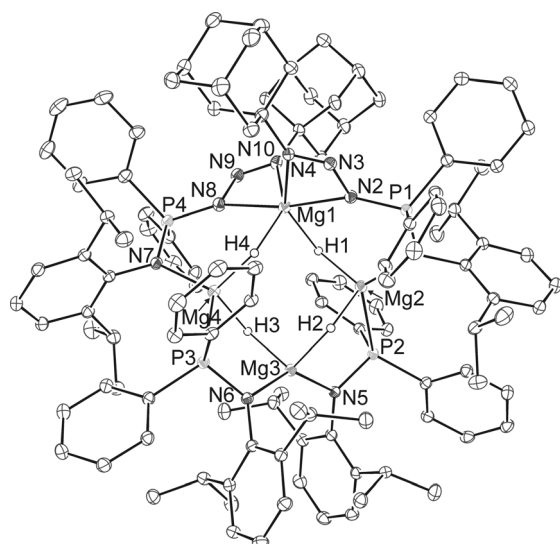
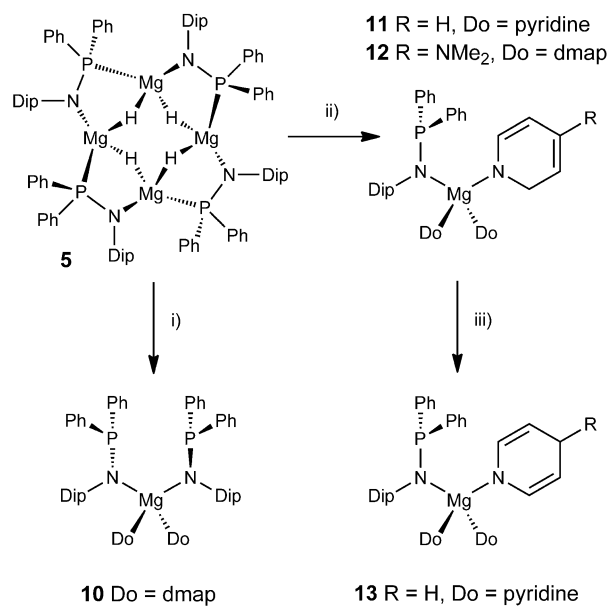


**Figure 3.** Molecular structure of **9** (30% thermal ellipsoids). Lattice solvent molecules and hydrogen atoms omitted, except hydride ligands. Only the main disordered parts of the adamantyl groups are shown. Selected bond lengths [Å] and angles [°]: P(1)–N(1) 1.6056(15), P(1)–N(2) 1.6495(15), P(2)–N(5) 1.6656(14), P(3)–N(6) 1.6588(15), P(4)–N(7) 1.6032(15), P(4)–N(8) 1.6501(16), N(2)–N(3) 1.366(2), N(3)–N(4) 1.268(2), N(8)–N(9) 1.365(2), N(9)–N(10) 1.267(2), Mg(1)–N(4) 2.2072(16), Mg(1)–N(10) 2.2274(17), Mg(1)–N(8) 2.2662(17), Mg(1)–N(2) 2.2700(16), Mg(3)–N(6) 2.0660(15), Mg(3)–N(5) 2.0675(16), Mg(4)–N(7) 2.0546(16), N(1)–Mg(2) 2.0549(15), P(2)–Mg(2) 2.6863(8), P(3)–Mg(4) 2.6775(8), Mg(1)–H(1) 1.88(2), Mg(1)–H(4) 1.88(2), Mg(2)–H(1) 1.81(2), Mg(2)–H(2) 1.79(2), Mg(3)–H(2) 1.85(2), Mg(3)–H(3) 1.87(2), Mg(4)–H(3) 1.84(2), Mg(4)–H(4) 1.78(2) (or: Mg–H: 1.78(2)–1.88(2)); N(8)–Mg(1)–N(2) 170.52(6), N(6)–Mg(3)–N(5) 139.29(6), N(7)–Mg(4)–P(3) 119.67(5), Mg–H–Mg ca. 118 (ave).

characterised as shown in Figure 4. Heating to 60 °C for 15 h lead to the clean rearrangement of **11** to the 1,4-dihydropyridide derivative **13** [LMg(py)<sub>2</sub>(1,4-dhp)] (Scheme 3). An analogous rearrangement is not possible for **12** under these conditions; a similar observation has previously been noted for other Group 2 metal–hydride systems.<sup>[12,13a]</sup> The molecular structure of **12** (Figure 4) shows a distorted tetrahedrally coordinated Mg<sup>2+</sup> ion, which binds to a terminal κ<sup>1</sup>-N-phosphinoamide ligand, a 4-dimethylamino-1,2-dihydropyridide ligand (from formal 1,2-addition of an MgH unit onto the DMAP pyridine ring), and two neutral, coordinating DMAP molecules. The shorter Mg–N distance of the dihydropyridide ligand compared with those of the neutral DMAP ligands, the C–C and C–N distances within the hydromagnesiated ring system, and the deviation from planarity of the CH<sub>2</sub> unit in question all support the designation of **12** as the 1,2-dihydropyridide product. NMR spectroscopic studies also support the clean 1,2-addition reaction to form complexes **11** and **12**, as well as the thermal conversion of **11** to **13**. Complex **11** shows a doublet ( $J_{H-H} = 4.0$  Hz) at  $\delta = 4.26$  ppm for the two hydrogen atoms of the 1,2-dihydropyridide unit in its <sup>1</sup>H NMR spectrum that converts to a centred multiplet for the two hydrogen atoms of the 1,4-dihydropyridide ligand at  $\delta = 4.03$  ppm (see Figures S35 and S41 in the Supporting Information).

We were also interested in the stoichiometric reactivity of non-enolisable ketones with **5**. Previously, Group 2 metal-hy-



**Scheme 3.** Stoichiometric reactivity of **5** with pyridines. i) 4 DMAP, toluene, 60 °C; ii) 12 pyridine or 12 DMAP, toluene, RT; iii) 60 °C (for Do = pyridine).

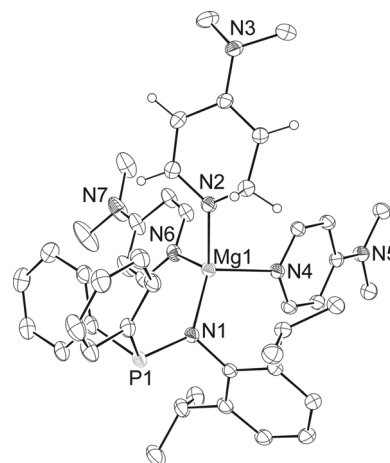


**Figure 4.** Molecular structure of **12** (30% thermal ellipsoids). A second, severely disordered molecule, lattice solvent and hydrogen atoms omitted, except hydrogens on the 1,2-dihydropyridide ligand. Selected bond lengths [Å] and angles [°]: P(1)–N(1) 1.6845(14), Mg(1)–N(2) 2.0198(16), Mg(1)–N(1) 2.0320(15), Mg(1)–N(4) 2.1279(15), Mg(1)–N(6) 2.1309(17), N(2)–C(25) 1.438(2), C(25)–C(26) 1.449(2), C(26)–C(27) 1.372(2), C(27)–C(28) 1.424(2), C(28)–C(29) 1.375(2), N(2)–C(29) 1.374(2); N(2)–Mg(1)–N(1) 123.63(6), N(4)–Mg(1)–N(6) 93.16(6).

dride complexes have been reported to undergo reductions of ketones,<sup>[8a,c,d,f-i,11e,13d,e]</sup> including older reports of less well-defined MgH species. The reaction of four equivalents of 2-adamantanone (2-AdO) with **5** mainly yielded the hydromagnesiated complex **14** [(L<sub>2</sub>Mg<sub>2</sub>(2-AdOH)<sub>2</sub>(2-AdO)] (Figure 5). The complex was structurally characterised, but because the overall data quality was poor, only an image is presented in the Supporting Information (Figure S55). The isolated product contains one hydrometallated ketone per magnesium centre and one coordinating ketone per Mg<sub>2</sub> unit. Repeating the reaction of **5** with six equivalents of 2-adamantanone showed that essential-

ly one product (**14**) was formed, which was isolated in moderate crystallised yield. Complex **14** contains two  $\text{Mg}^{2+}$  cations that are bridged by two 2-adamantanolate ligands from hydromagnesiation of 2-adamantanone, and is further bridged by a  $\kappa^2$ -*P,N*-phosphinoamide ligand. In addition, one terminal  $\kappa^1$ -*N*-phosphinoamide coordinates to one Mg centre, and the other Mg centre is coordinated by one neutral 2-adamantanone molecule. In deuterated benzene solution at room temperature, two very broad resonances ( $\delta=32$  and 42 ppm) are found in the  $^{31}\text{P}$  NMR spectrum of **14** corresponding to the two phosphinoamide ligands. At elevated temperatures, these merge to one broad resonance ( $\delta=37.8$  ppm at 65 °C) and, accordingly, one septet and one doublet are found for the isopropyl groups of the phosphinoamide ligands in the  $^1\text{H}$  NMR spectrum at this temperature (Figure S45 in the Supporting Information), showing fluxional ligand exchange processes under these conditions.

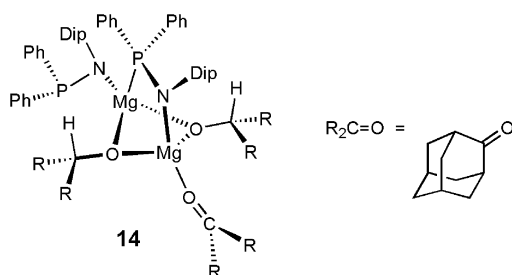


**Figure 5.** Chemical drawing of  $[(\text{L}_2\text{Mg}_2(2\text{-AdOH})_2(2\text{-AdO}))]$  **14**. For an image from a crystal structure determination, see Figure S55 in the Supporting Information.

### Catalytic reactivity

Considering the recent success of employing alkaline earth metal-hydride complexes as (pre)catalysts for the hydroboration or hydrosilylation of unsaturated molecules,<sup>[10]</sup> we wanted to investigate the applicability of complex **5** in similar catalytic conversions. We reasoned that complexes such as **5**, stabilised by a ligand that favours bridging and terminal coordination modes, can deliver open and reactive “LMgH” fragments, and potentially act as a highly active (pre)catalyst for these reactions.

### Hydroboration and hydrosilylation of ketones

Since Mg-catalysed hydroborations of aldehydes and ketones with pinacolborane (HBPin) have previously been reported,<sup>[10,11d,21]</sup> and considering the rapid hydromagnesiation of 2-adamantanone (2-AdO) with **5** to yield **14**, we chose 2-adamantanone and benzophenone as simple and symmetric substrates. Notably, various side-reactions (enolisation and deprotonation, aldolcondensation) are unlikely or impossible here, and such substrates kept the identification of products and intermediates simple for this study. Remarkably, we found that reactions of either ketone with 1.2 equivalents of HBPin in  $\text{C}_6\text{D}_6$  at room temperature were complete in under 7 min after addition of the magnesium hydride cluster **5** (0.5 mol% of tetra-

mer, 2.0 mol% Mg) (Table 1). The catalyst loading for reactions of HBPin with 2-AdO could even be reduced to 0.05 mol% (0.2 mol% Mg) without suffering any loss of activity, whereas the hydroboration yield for  $\text{Ph}_2\text{CO}$  dropped slightly to 88% over 15 min when the catalyst loading was decreased to 0.05 mol% (Table 1, entries 1 and 2). These two cases correspond to turnover frequencies (TOFs) of  $>4243\text{ h}^{-1}$  and  $1760\text{ h}^{-1}$  per Mg centre, respectively (or  $>16970\text{ h}^{-1}$  and  $7040\text{ h}^{-1}$  per molecule **5**), which is remarkable even for transition metal-catalysed hydroborations of ketones.<sup>[10d]</sup> We also tested derivatives of **5** described above. The PMDETA adduct **8** performed equally as well as **5** for the hydroboration of 2-adamantanone (entry 4) with rapid and complete conversion at room temperature at low catalyst loading despite only having two Mg and hydride centres (TOF:  $>8486\text{ h}^{-1}$  per Mg or  $>16970\text{ h}^{-1}$  per molecule). This suggests that the possible lower (pre)catalyst loading limit of **5** or **8** for this specific reaction could even be further reduced, though it becomes increasingly difficult to accurately perform this with small-scale reactions, as well as avoid partial (pre)catalyst decomposition. The performance of the phosphinoamide/phosphazide complex **9** on the other hand is significantly poorer with 50% conversion observed after 60 min, and 84% conversion after 130 min (entry 5). Thus, this system was not further explored. We also tested the homoleptic phosphinoamide complex **1** (vide infra for a discussion), and found that it performed equally as well as our best results (entry 6).

After successful hydroboration, the  $^1\text{H}$  NMR spectra of the reaction mixtures showed new resonances at approximately 4.44 ppm (2-AdO) or 6.44 ppm ( $\text{Ph}_2\text{CO}$ ), consistent with the presence of a proton on the former carbonyl carbon atom. Singlets at 1.08 ppm (2-AdO) or 0.98 ppm ( $\text{Ph}_2\text{CO}$ ), which integrated to 12H and were slightly shifted in comparison to the HBPin starting material, were also observed and assigned to the twelve methyl protons of the resulting borate esters, (2-Ad(H)O)BPIn or ( $\text{Ph}_2\text{C(H)O}$ )BPIn. The presence of these products was further confirmed by  $^{11}\text{B}$  NMR spectroscopy.<sup>[12d,22]</sup>

Encouraged by these promising results, we investigated catalytic reductions of these ketones by a silane as the hydride source (Table 1).<sup>[23]</sup> To the best of our knowledge, only one example of a magnesium-catalysed hydrosilylation has been reported to date, which is the 1,4-addition of  $\text{Ph}_2\text{SiH}_2$  to  $\alpha,\beta$ -unsaturated esters in the presence of a sterically demanding magnesium hydridoborate.<sup>[24]</sup> Thus, we attempted the hydrosilylation of our previous two substrates with  $\text{PhSiH}_3$  in varying stoichiometries in the presence of catalytic amounts of **5**. Initial studies revealed that treatment of benzophenone with phenylsilane in  $\text{C}_6\text{D}_6$  at 70 °C with 1.5 mol% of compound **5** produces the dialkoxysilane,  $\text{Ph(H)Si(OCHPh)}_2$ , as the major product, which was also observed for hydrosilylations of ketones using a calcium-hydride catalyst.<sup>[13d]</sup> The silane/ketone ratio was therefore chosen to be approximately 1:2 for all further reactions (Table 1, entries 7–10). After 24 h at room temperature, only very small amounts of the dialkoxysilane were present, as judged by  $^1\text{H}$  NMR spectroscopy. The spectrum mainly showed unreacted  $\text{PhSiH}_3$  and  $\text{Ph}_2\text{CO}$ . Heating accelerated the hydrosilylation significantly such that after 22 h at 50 °C more than

**Table 1.** Hydroelementations of ketones catalysed by compounds **1**, **5**, **8** and **9**.

Entry	Catalyst loading [mol %] <sup>[a]</sup>	Ketone	Hydride source	T [°C]	t	Conversion [%] <sup>[b]</sup>	TOF [h <sup>-1</sup> ] <sup>[c]</sup>	Main product <sup>[d]</sup>
1	0.05, <b>5</b>	2-adamantanone	HBPIn	25	< 7 min	> 99	> 4243	R'BPIn
2	0.05, <b>5</b>	benzophenone	HBPIn	25	15 min	88	1760	RBPIn
3	0.5, <b>5</b>	benzophenone	HBPIn	25	< 7 min	> 99	> 424	RBPIn
4	0.05, <b>8</b>	2-adamantanone	HBPIn	25	< 7 min	> 99	> 8486	R'BPIn
5	0.05, <b>9</b>	2-adamantanone	HBPIn	25	130 min	84	194	R'BPIn
6	0.05, <b>1</b>	2-adamantanone	HBPIn	25	< 7 min	> 99	> 8486	R'BPIn
7	1.5, <b>5</b>	2-adamantanone	PhSiH <sub>3</sub>	70	15 min	> 99 <sup>[e]</sup>	66	R' <sub>2</sub> Si(H)Ph
8	1.5, <b>5</b>	benzophenone	PhSiH <sub>3</sub>	70	50 h	93	0.31	R' <sub>2</sub> Si(H)Ph
9	1.5, <b>8</b>	2-adamantanone	PhSiH <sub>3</sub>	70	15 min	> 99 <sup>[e]</sup>	132	R' <sub>2</sub> Si(H)Ph
10	1.5, <b>1</b>	2-adamantanone	PhSiH <sub>3</sub>	70	15 min	> 99 <sup>[e]</sup>	132	R' <sub>2</sub> Si(H)Ph
11	1.5, <b>5</b>	2-adamantanone	Ph <sub>2</sub> SiH <sub>2</sub>	80	15 h	< 3	-	-

[a] Based on full molecules **1**, **5**, **8** or **9**; for **1** and **8** two times higher per Mg centre; for **5** and **9** four times higher per Mg centre; [b] the reaction was monitored using <sup>1</sup>H NMR spectroscopy and conversion yields were determined by integration of the proton on the former carbonyl-C atom against an internal standard; [c] calculated per Mg centre; TOF are double for molecules **1** and **8**, and four times the value for molecules **5** and **9**; [d] represents > 90% of total products, R = Ph<sub>2</sub>C(H)O<sup>-</sup>, R' = 2-adamantanolate; [e] hydrosilylations of 2-adamantanone produced a small quantity of white precipitate at elevated temperatures after longer reaction times than given that appears to reduce the measured conversion in solution, likely due to R'<sub>3</sub>SiPh product precipitation.

50% of the ketone had been transformed into the alkoxide. Increasing the temperature to 70 °C produced 73% conversion after 24 h and 93% conversion after 50 h (entry 8). On the other hand, hydrosilylation of 2-adamantanone with PhSiH<sub>3</sub> proceeded much more rapidly than the hydrosilylation of benzophenone under similar conditions. After 15 min at 70 °C with 1.5 mol% of **5**, more than 99% of 2-AdO had been transformed into 2-adamantanolate (entry 7), and the same could be achieved using complex **8** (entry 9). Here, the product ratios were approximately 70% R'<sub>2</sub>Si(H)Ph (R' = 2-adamantanolate) versus 30% R'<sub>3</sub>SiPh using complex **5** (entry 7) and a ratio of approximately 88:12 for the respective reaction with catalyst **8** (entry 9). This ratio quickly changes to favour R'<sub>3</sub>SiPh with continued heating. Because no further ketone conversion was possible, this points to a dismutation reaction from R'<sub>2</sub>Si(H)Ph to R'<sub>3</sub>SiPh. The preferred product in these latter conversions (R'<sub>3</sub>SiPh) is the trialkoxysilane, as opposed to the dialkoxysilane when benzophenone is used as the ketone. Catalytic reduction of 2-adamantanone was not observed in the presence of **5** with diphenylsilane as the hydride source (entry 11). Once again, investigating complex **1** in this reaction (entry 10) shows that it performs equally as well as the best magnesium hydride compounds tested by us. Complexes **1** and **8** achieved a turnover frequency of 132 h<sup>-1</sup> per Mg centre, or 264 h<sup>-1</sup> per molecule.

We noticed throughout experiments involving magnesium-hydride **5**, that all characteristic NMR spectroscopic resonances of the magnesium-hydride compound had disappeared during or by the end of the catalysis, especially when the samples were heated. Instead, these provided new sharp <sup>1</sup>H NMR resonances assigned to the compounds LBPIn **15** (<sup>31</sup>P{<sup>1</sup>H} NMR: 58.8 ppm, <sup>11</sup>B{<sup>1</sup>H} NMR: 25.1 ppm), or PhSiH<sub>2</sub>L **7** (<sup>31</sup>P{<sup>1</sup>H} NMR: 61.7 ppm) as the L-containing products. Merely in the fastest hydroboration reactions with catalyst loadings ≥ 2.5 mol% was cluster **5** still identifiable a few minutes after full conversion of the substrate into the alkoxide, though in much lower concentrations than at the start. Under catalytic conditions, complex **5**

is transformed to the phosphinoamide-containing borane **15**, or silane **7**, and presumably, to soluble and catalytically active magnesium-hydride species. The presence of low concentrations of **5** in isolated cases where high catalyst loadings are used can be explained by the fast conversion and the fact that not all of compound **5** needs to act as the (pre)catalyst.

### Hydroboration and hydrosilylation of pyridine

In light of the successful stoichiometric reactivity of **5** with pyridines (Scheme 3) and previously reported magnesium-hydride complexes,<sup>[5c,7a,d,8b,12]</sup> we studied the respective catalytic hydroboration and hydrosilylation of pyridine using **5**. Equimolar amounts of pyridine and HBPIn were treated with 2.5 mol% of **5** (10 mol% Mg) in deuterated benzene and, as expected, complex **5** is immediately consumed. The catalytic hydroboration of pyridine is possible at elevated temperatures, albeit slow and incomplete. After 48 h at 70 °C, 32% of total dihydropyridide products, PinBdhp (dhp = dihydropyridide), have been formed, with 87.5% being the 1,4-dhp versus 12.5% of 1,2-dhp. Modification of the reaction temperature to 80 °C gives 35% conversion after 24 h (89% 1,4-dhp:11% 1,2-dhp) and 58% conversion after 96 h (93% 1,4-dhp:7% 1,2-dhp). Increasing the catalyst loading to 5 mol% of **5** results in slightly higher yields of hydroborated pyridine (53.5% after 37 h at 70 °C). Full conversion of pyridine into PinBdhp is not achieved because pinacolborane slowly decomposes to B<sub>2</sub>(Pin)<sub>3</sub> during the course of this reaction,<sup>[11d,12]</sup> a byproduct which could be isolated from one of the catalysis experiments as a crystalline product. In addition, the <sup>11</sup>B NMR spectra, taken after heating the reaction mixture at 70 or 80 °C for at least 15 h, show a broad peak at around 22 ppm that was attributed to B<sub>2</sub>Pin<sub>3</sub> and a quartet at -11 ppm for py·BH<sub>3</sub>. Both of these peaks increase in intensity with prolonged heating of the samples, indicating the continued decomposition of HBPIn under the employed conditions.

Similarly, catalytic hydrosilylation of pyridine with 2.5 mol% of **5** is possible, but is slow and does not go to completion. Upon addition of **5** to a mixture of pyridine and  $\text{PhSiH}_3$  at room temperature,  $[\text{LMg}(\text{py})_2(1,2\text{-dhp})]$  **11** is formed immediately, which is also the kinetic product in stoichiometric reactions of **5** with excess pyridine (vide supra). More forcing conditions are needed to achieve any catalytic conversion. After 48 h at  $80^\circ\text{C}$ , only around 52% of pyridine has been transformed into a dihydropyridide species with  $[(1,4\text{-dhp})_2\text{PhSiH}]$  being the main product, though the exact product distribution is unknown, as  $[(1,4\text{-dhp})_2\text{PhSiH}]$ ,  $[(1,2\text{-dhp})_2\text{PhSiH}]$ , and  $[(1,4\text{-dhp})(1,2\text{-dhp})\text{PhSiH}]$  are all formed alongside each other showing overlapping  $^1\text{H}$  NMR resonances. The phosphinoamide-containing component at the end of the reaction is yet again **7**.

### Mechanistic considerations

The proposed mechanism for the catalytic hydroboration and hydrosilylation of ketones for several previously reported systems often follows a general insertion/ $\sigma$ -bond metathesis cycle,<sup>[10,23]</sup> although other possibilities remain. To shed light on the mechanism using the phosphinoamide-magnesium complexes reported here (**1**, **5** and **8**), and to identify the possible active species, we performed some stoichiometric reactions to assess the feasibility of individual steps for this mechanism. Complex **5** reacts rapidly with 2-adamantanone to give the insertion product **14** as previously stated (Figure 5). Similarly, **5** readily reacts with benzophenone in a hydromagnesiation reaction, as judged by in situ  $^1\text{H}$  NMR spectroscopic data. No well-defined products could be isolated from the latter reaction mixtures, and the formed complexes likely depend on the  $\text{Mg}:\text{Ph}_2\text{CO}$  ratio including coordination of unreacted benzophenone. These findings support that  $\text{C}=\text{O}$  insertion into the  $\text{MgH}$  moiety could be the first step in the catalytic cycle.

The reaction of **5** with HBPin alone in deuterated benzene is very slow, and the starting materials remain largely unreacted for a few days, although some **15** is produced eventually, and later other compounds including LH. Although a large excess of HBPin is typically used in catalytic studies, reactions of **5** with unsaturated substrates such as ketones were found to be very rapid in comparison. The treatment of complex **5** with  $\text{PhSiH}_3$  in deuterated benzene at elevated temperature in the absence of donor molecules or substrates showed no reaction. Complex **5** alone is furthermore stable towards heat in the solid state, in non-coordinating solvents and towards excess phosphinoamine proligand LH; that is, none of complex **1** is formed, even at elevated temperatures, to our surprise. Furthermore, it does not appear to react at room temperature with unsaturated organic molecules lacking good donor atoms. Consequently, the ketone addition must play a role in removing L from magnesium, and in the formation of **15** and **7**. Hydromagnesiation of  $\text{LMgH}$  units with ketones forms hard alcoholate ligands that bind strongly to hard  $\text{Mg}^{2+}$  ions, likely labilising the  $\text{Mg}$ -phosphinoamide bonds, and inducing ligand-exchange processes. Additionally, the excess unreacted ketone can act as additional donor molecules, and presumably induce equilibria similar to those found when **5** is dissolved in THF

(see the previous section and Figures S21 and S22 in the Supporting Information). This is also illustrated by ligand rearrangements in the molecular structure of **8** compared with compound **5**. Given the highly symmetrical solution NMR spectra found for **1** that suggest flexible solution dynamics (vide supra) we also reacted this compound with four equivalents of HBPin, and found that it reacted rapidly at room temperature to form **15** (Figures S49–S51 in the Supporting Information). By implication, freshly generated “ $\text{MgH}_2$ ” may be the byproduct, though this could not be spectroscopically verified. A broad resonance at approximately 1.5 ppm in the  $^1\text{H}$  NMR spectrum (Figure S49) could be attributed to a new reactive species. The fast ligand-loss from **1** when treated with HBPin, especially compared to the very slow reaction of **5** with HBPin, and the fact that the phosphinoamide ligands in our catalytic studies of **5** and **8** eventually end up in **7** or **15**, led us to test **1** as a catalyst, which yielded the equal-best results.

Next, we treated complex **14** with 2.5 equivalents of HBPin or  $\text{PhSiH}_3$  to investigate whether our ketone insertion product can easily undergo  $\sigma$ -bond metathesis with each hydride source. Compound **14** and HBPin react instantaneously to give the borate ester 2-Ad(H)OBPin and **15**, and the resonances of the starting materials have completely vanished from multinuclear NMR spectra of the reaction mixtures. The fate of the Mg moiety is unknown, and NMR spectroscopic experiments suggest that the magnesium hydride complex **5** is not reformed in detectable quantities after release of the hydroborated product (vide supra). A reaction of complex **14** with  $\text{PhSiH}_3$  at room temperature was not observed. However, within several minutes at  $70^\circ\text{C}$ , complex **14** is consumed, alkoxy silanes form, and the phosphinoamide groups are present as **7**. The rapid formation of Ad(H)OBPin from **14** at room temperature when treated with pinacolborane, and the comparable reaction of **14** with phenylsilane at an elevated temperature gives credibility to a general insertion/ $\sigma$ -bond metathesis mechanism. Importantly, the conditions and reaction rates of the  $\sigma$ -bond metathesis of the alcoholate complex **14** with the hydride source (HBPin or  $\text{PhSiH}_3$ ) correlate with the best observed catalysis conditions of the respective reaction, and thus, may correspond to the rate-determining step in the mechanism.

The stoichiometric chemistry reported in the previous sections already shows several possibilities, such as donor-induced (THF, PMDETA) rearrangements and redistributions. Catalytic reactions with an excess of unsaturated organic substrates (e.g., ketones, pyridines) possessing good donor atoms (O, N), likely induce a series of equilibria to generate compounds of the type  $[\{\text{LMg}(\text{Do})_n\text{H}\}_m]$  **A** [Scheme 4A, Eq. (1)], that could be active catalytic species. The donor species (Do) can be neutral donor groups such as  $\text{R}_3\text{P}$  (from  $\text{L}^-$ ), the large excess of substrates such as ketones (or pyridines) under catalytic regimes, and even the generated reaction products (e.g.,  $\text{PhSiH}(\text{OR})_2$ ). Depending on the donor properties and concentrations, several aggregates can be present in solution. As previously observed, for example by dissolving **5** in THF, Schlenk-like equilibria with numerous redistribution possibilities [formulated in a simplified form as Eq. (2)], could rapidly form donor-stabilised and soluble  $\text{MgH}_2$  complexes such as **B**. That these equili-

bria are important may be supported by the fact that both **1** and **8** performed equally as well as **5** in catalytic hydroborations and hydrosilylations of ketones. Complex **8** is a donor adduct of **5** and appears to have the potentially active complex  $[(\text{PMDETA})\text{MgH}_2]$  preorganised in its molecular structure (see Figure 3): only a long Mg–P coordination bond and two bridging hydride...Mg contacts have to be invested to release an  $\text{L}_2\text{Mg}$  fragment and form  $[(\text{PMDETA})\text{MgH}_2]$ , which may be aided by additional present donor molecules. The more sterically shielded and chemically robust complex **9** was a significantly less effective (pre)catalyst by comparison.

All of these considerations lead to a range of Mg-complex possibilities with various donors and monoanionic ligands ( $\text{L}^{\text{gen-}}$ ). The ligand  $\text{L}^{\text{gen-}}$  can be any general monoanionic ligand that is likely to exist in these reaction mixtures, such as  $\text{L}^-$ ,  $\text{R}_2\text{CHO}^-$  (from direct hydromagnesiations), and/or  $\text{H}^-$ . Because the phosphinoamide moiety  $\text{L}^-$  is bound to boron or silicon as **7** or **15** at the end of the reaction, and **5** does not rapidly react with the stoichiometric hydride sources EH ( $\text{E} = \text{BPin}$ ,  $\text{PhSiH}_2$ ), a more active magnesium complex, simplified as  $[\text{L}^{\text{gen}}\text{Mg}(\text{Do})_n\text{L}]$ , likely reacts with EH to form a magnesium hydride complex **C** and the final phosphinoamide species **7** or **15** [Scheme 4A, Eq. (3)]. This key step is further supported by the rapid reaction of **1** with HBpin to generate **15** and likely an active “ $\text{MgH}_2$ ” complex (e.g., **B**) in a similar fashion to Equation (3) in Scheme 4. Therefore, the catalytic properties of **1** may be approaching those of freshly generated and solubi-

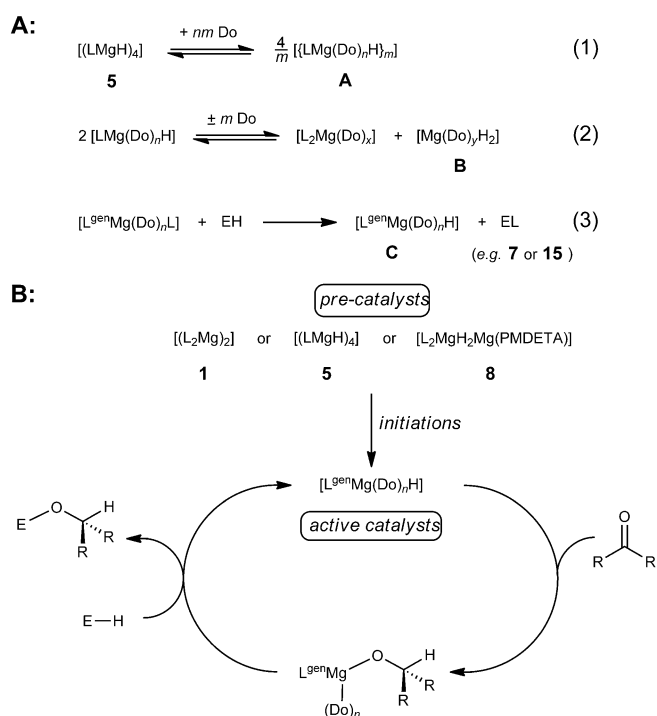
lised “ $\text{MgH}_2$ ”. Ligand-exchange reactions of species such as **A–C**, as well as coordination and aggregation processes would further allow access to a large number of possible active complexes present in actual reaction mixtures of catalytic preparations.

The active catalysts obtained after the initiation steps outlined above likely undergo the hydrometallation/ $\sigma$ -bond metathesis cycle previously proposed for other systems (Scheme 4B), which has support from our stoichiometric investigations: both the hydrometallation and the  $\sigma$ -bond metathesis steps are possible, and show the appropriate rates under the respective conditions. At this stage, we cannot discount other mechanistic possibilities, and evidence for slightly different mechanistic pathways has been forthcoming for related zinc and calcium systems. In comparison, it has been found that hydrosilylations of carbonyl complexes can already be successfully catalysed at room temperature for a series of heteroleptic, ligand-stabilised zinc-hydride complexes.<sup>[25,26]</sup> For one of these examples, an associative mechanism with a silane/zinc-hydride adduct as the active species has been proposed.<sup>[26e]</sup> For  $\beta$ -diketiminato-calcium-hydride-catalysed ketone hydrosilylations, a concerted mechanism via a hypercoordinated hydridosilicate species was suggested.<sup>[10,13d]</sup> Also, a simple hydroboration or hydrosilylation mechanism on a Lewis acid activated ketone cannot be completely ruled out.

## Conclusions

We have presented the synthesis and interconversion of a series of magnesium(II) complexes bearing the sterically demanding phosphinoamide ligand  $\text{Ph}_2\text{PNDip}^- (\text{L}^-)$ . Reactions of LH with  $\text{Mg}(\text{nBu})_2$  afforded the complexes **1**  $[(\text{L}_2\text{Mg})_2]$  and **2**  $[\text{L}_3\text{Mg}_2(\text{nBu})]$ , and reactions with added  $\text{PhSiH}_3$  at elevated temperatures yielded the hydride complexes **4**  $[(\text{L}_2\text{Mg}_2(\text{nBu})\text{H})_2]$  and **5**  $[(\text{LMgH})_4]$ , as well as the hexamer **6**  $[(\text{LMgH})_6]$ . Complex **5** was studied for its stoichiometric reactivity, and afforded the MgH-complex derivatives  $[(\text{L}_2\text{MgH}_2\text{Mg}(\text{PMDETA}))]$  **8** and  $[\text{L}'\text{L}'_2\text{Mg}_4\text{H}_4]$  **9** ( $\text{L}' = \text{DipNP}(\text{N}_3\text{Ad})\text{Ph}_2$ ), with the latter being obtained by transformation of two phosphinoamides with  $\text{AdN}_3$  into phosphazide ligands. Several complexes have an overall ring shape such as **4**, **5**, **6** and **9**, and the solid-state structures are dominated by bridging as well as terminal phosphinoamide ligands. Both head/head and head/tail phosphinoamide orientations have been found in aggregated complexes. Solution studies generally revealed symmetric geometries indicating flexible phosphinoamide coordination, with the exception of the *n*-butyl-bridged complexes **2** and **4**, which show retention of the overall solid-state geometries and partially suppressed ligand-exchange processes.

Further stoichiometric reactivity of **5** with pyridines yielded an example of selective generation of a 1,2- versus a 1,4- hydromagnesiation product with pyridine. The complexes  $[\text{L}_2\text{Mg}(\text{dmap})_2]$  **10**,  $[\text{LMg}(\text{py})_2(1,2\text{-dhp})]$  **11**,  $[\text{LMg}(\text{dmap})_2(1,2\text{-dadhp})]$  **12**, and  $[\text{LMg}(\text{py})_2(1,4\text{-dhp})]$  **13** are described. Complex **5** was found to rapidly hydromagnesiate ketones and afforded, for example, the alcoholate complex  $[(\text{L}_2\text{Mg}_2(2\text{-AdOH})_2(2\text{-AdO}))]$  **14**.



**Scheme 4.** A: Possible precatalyst activation reactions (1)–(3), simplified; B: proposed simplified catalytic cycles for the hydroelementation of ketones with precatalyst **1**, **5** or **8**. *n*, *m*, *x* and *y* are small natural numbers,  $\text{L}^{\text{gen-}}$  = monoanionic ligand such as  $\text{L}^-$ ,  $\text{R}_2\text{CHO}^-$ ,  $\text{H}^-$ , etc., Do = (neutral) donor group, such as  $\text{R}_3\text{P}$  (from  $\text{L}^-$ ), substrates such as ketones, reaction products, R = organic substituent, EH = borane or silane fragment.

Extending the study to catalytic transformations revealed that complexes **1**, **5** and **8** are highly active precatalysts for the hydroboration of ketones at room temperature with very low catalyst loadings. Respective ketone hydrosilylations can also be achieved rapidly at elevated temperatures. The sterically more shielded complex **9** shows a much lower stoichiometric reactivity and was a poorer catalyst. For example, the reaction of pinacolborane with 2-adamantanone catalysed by complexes **1** and **8** is rapid at room temperature with a turnover frequency of  $>8485\text{ h}^{-1}$  per Mg centre ( $>16970\text{ h}^{-1}$  per molecule). The hydrosilylation of 2-adamantanone with phenylsilane catalysed by complexes **1** and **8** proceeds in about 15 min at  $70^\circ\text{C}$ , with a turnover frequency of  $132\text{ h}^{-1}$ . Also, catalytic hydroboration and hydrosilylation of pyridine was possible, but required elevated temperatures and long reaction times, and only provided partial conversion. Our studies suggest that complexes **1**, **5** and **8** are precursors to the active catalysts in these systems and likely generate highly active MgH-complexes in situ. The results are supportive of an insertion/ $\sigma$ -bond-metathesis-type mechanism for the hydroelementation of ketones, with the  $\sigma$ -bond metathesis step likely being rate-determining. Catalytic reactions of **1** with hydride sources such as HBPIn may represent those of freshly generated, highly active and soluble, parent "MgH<sub>2</sub>", and will likely find further applications in synthesis and catalysis.

## Experimental Section

Full experimental details can be found in the Supporting Information.

CCDC 1457545 (**1**), 1457546 (**4-C<sub>6</sub>H<sub>14</sub>**), 1457547 (**9·6 C<sub>6</sub>H<sub>6</sub>**), 1457548 (**8·2 C<sub>7</sub>H<sub>8</sub>**), 1457549 (**6·3 C<sub>6</sub>H<sub>6</sub>**), 1457550 (**3·7 C<sub>6</sub>H<sub>14</sub>**), 1457551 (**12·5 C<sub>6</sub>H<sub>14</sub>**), 1457552 (**2·1.5 C<sub>5</sub>H<sub>12</sub>**) and 1457553 (**5·C<sub>6</sub>H<sub>14</sub>**) contain the supplementary crystallographic data for this paper. These data are provided free of charge by The Cambridge Crystallographic Data Centre.

## Acknowledgements

A.S. is grateful to the Australian Research Council for project support and a fellowship. Part of this research was undertaken on the MX1 and MX2 beamlines at the Australian Synchrotron, Victoria, Australia.

**Keywords:** hydrides · hydroboration · hydromagnesiation · hydrosilylation · magnesium

- [1] a) H. Kohlmann, *Metal Hydrides*, Encyclopedia of Physical Sciences and Technology, 3rd ed. (Ed.: R. A. Meyers), Academic Press, **2002**, 9, 441–458; b) W. Grochala, P. P. Edwards, *Chem. Rev.* **2004**, *104*, 1283–1315; c) S. Aldridge, A. J. Downs, *Chem. Rev.* **2001**, *101*, 3305–3365; d) H. D. Kaesz, R. B. Saillant, *Chem. Rev.* **1972**, *72*, 231–281; e) *Metal hydrides* (Eds.: W. M. Mueller, J. P. Blackledge, G. G. Libowitz), Academic Press, New York, **1968**.
- [2] S. Harder, *Chem. Commun.* **2012**, *48*, 11165–11177.
- [3] L. Fohlmeister, A. Stasch, *Aust. J. Chem.* **2015**, *68*, 1190–1201.
- [4] M. S. Holzwarth, B. Plietker, *ChemCatChem* **2013**, *5*, 1650–1679.
- [5] a) R. Lalrempuia, C. E. Kefalidis, S. J. Bonyhady, B. Schwarze, L. Maron, A. Stasch, C. Jones, *J. Am. Chem. Soc.* **2015**, *137*, 8944–8947; b) M. Arrow-

- smith, B. Maitland, G. Kociok-Köhn, A. Stasch, C. Jones, M. S. Hill, *Inorg. Chem.* **2014**, *53*, 10543–10552; c) S. Harder, J. Spielmann, J. Intemann, *Dalton Trans.* **2014**, *43*, 14284–14290; d) J. Intemann, J. Spielmann, P. Sirsch, S. Harder, *Chem. Eur. J.* **2013**, *19*, 8478–8489; e) S. Harder, J. Spielmann, J. Intemann, H. Bandmann, *Angew. Chem. Int. Ed.* **2011**, *50*, 4156–4160; *Angew. Chem.* **2011**, *123*, 4242–4246; f) S. J. Bonyhady, D. Collis, G. Frenking, N. Holzmann, C. Jones, A. Stasch, *Nat. Chem.* **2010**, *2*, 865–869; g) S. J. Bonyhady, C. Jones, S. Nembenna, A. Stasch, A. J. Edwards, G. J. McIntyre, *Chem. Eur. J.* **2010**, *16*, 938–955; h) S. P. Green, C. Jones, A. Stasch, *Angew. Chem. Int. Ed.* **2008**, *47*, 9079–9083; *Angew. Chem.* **2008**, *120*, 9219–9223.
- [6] a) D. J. Liptrot, M. S. Hill, M. F. Mahon, *Chem. Eur. J.* **2014**, *20*, 9871–9874; b) D. V. Graham, A. R. Kennedy, R. E. Mulvey, C. T. O'Hara, *Acta Crystallogr. Sect. C* **2006**, *62*, m366–m368; c) P. C. Andrikopoulos, D. R. Armstrong, A. R. Kennedy, R. E. Mulvey, C. T. O'Hara, R. B. Rowlings, *Eur. J. Inorg. Chem.* **2003**, 3354–3362; d) D. J. Gallagher, K. W. Henderson, A. R. Kennedy, C. T. O'Hara, R. E. Mulvey, R. B. Rowlings, *Chem. Commun.* **2002**, 376–377.
- [7] a) S. Schnitzler, T. P. Spaniol, L. Maron, J. Okuda, *Chem. Eur. J.* **2015**, *21*, 11330–11334; b) D. Martin, K. Beckerle, S. Schnitzler, T. P. Spaniol, L. Maron, J. Okuda, *Angew. Chem. Int. Ed.* **2015**, *54*, 4115–4118; *Angew. Chem.* **2015**, *127*, 4188–4191; c) R. Lalrempuia, A. Stasch, C. Jones, *Chem. Asian J.* **2015**, *10*, 447–454; d) H. Xie, X. Hua, B. Liu, C. Wu, D. Cui, *J. Organomet. Chem.* **2015**, *798*, 335–340; e) M. Arrowsmith, M. S. Hill, D. J. MacDougall, M. F. Mahon, *Angew. Chem. Int. Ed.* **2009**, *48*, 4013–4016; *Angew. Chem.* **2009**, *121*, 4073–4076.
- [8] Selected references for the chemistry of less well-defined MgH complexes: a) A. B. Goel, E. C. Ashby, *J. Organomet. Chem.* **1981**, *214*, C1–C6; b) E. C. Ashby, A. B. Goel, *J. Organomet. Chem.* **1981**, *204*, 139–145; c) E. C. Ashby, A. B. Goel, R. N. DePriest, *J. Am. Chem. Soc.* **1980**, *102*, 7779–7780; d) E. C. Ashby, A. B. Goel, *Inorg. Chem.* **1979**, *18*, 1306–1311; e) E. C. Ashby, A. B. Goel, *Inorg. Chem.* **1978**, *17*, 322–326; f) E. C. Ashby, J. J. Lin, A. B. Goel, *J. Org. Chem.* **1978**, *43*, 1564–1566; g) E. C. Ashby, J. J. Lin, A. B. Goel, *J. Org. Chem.* **1978**, *43*, 1560–1563; h) E. C. Ashby, J. J. Lin, A. B. Goel, *J. Org. Chem.* **1978**, *43*, 1557–1560; i) E. C. Ashby, A. B. Goel, J. J. Lin, *Tetrahedron Lett.* **1977**, *18*, 3133–3136; j) E. C. Ashby, A. B. Goel, *J. Org. Chem.* **1977**, *42*, 3480–3485; k) E. C. Ashby, A. B. Goel, *Inorg. Chem.* **1977**, *16*, 2941–2944; l) E. C. Ashby, A. B. Goel, *Inorg. Chem.* **1977**, *16*, 2082–2085; m) E. C. Ashby, A. B. Goel, *Inorg. Chem.* **1977**, *16*, 1441–1445; n) E. C. Ashby, A. B. Goel, *J. Chem. Soc., Chem. Commun.* **1977**, 169; o) E. C. Ashby, R. Arnott, S. Srivatsava, *Inorg. Chem.* **1975**, *14*, 2422–2426; p) E. C. Ashby, R. G. Beach, *Inorg. Chem.* **1971**, *10*, 906–910.
- [9] a) V. Leich, T. P. Spaniol, L. Maron, J. Okuda, *Angew. Chem. Int. Ed.* **2016**, *55*, 4794–4797; *Angew. Chem.* **2016**, *128*, 4872–4876; b) V. Leich, T. P. Spaniol, J. Okuda, *Inorg. Chem.* **2015**, *54*, 4927–4933; c) P. Jochmann, J. P. Davin, T. P. Spaniol, L. Maron, J. Okuda, *Angew. Chem. Int. Ed.* **2012**, *51*, 4452–4455; *Angew. Chem.* **2012**, *124*, 4528–4531; d) S. Harder, J. Brettar, *Angew. Chem. Int. Ed.* **2006**, *45*, 3474–3478; *Angew. Chem.* **2006**, *118*, 3554–3558.
- [10] For recent reviews, see: a) M. Arrowsmith, *Encycl. Inorg. Bioinorg. Chem.* **2016**, DOI: 10.1002/9781119951438.eibc2299; b) M. S. Hill, D. J. Liptrot, C. Weetman, *Chem. Soc. Rev.* **2016**, *45*, 972–988; c) R. Rochat, M. J. Lopez, H. Tsurugi, K. Mashima, *ChemCatChem* **2016**, *8*, 10–20; d) C. C. Chong, R. Kinjo, *ACS Catal.* **2015**, *5*, 3238–3259; e) K. Revunova, G. I. Nikonov, *Dalton Trans.* **2015**, *44*, 840–866; f) M. R. Crimmin, M. S. Hill, *Top. Organomet. Chem.* **2013**, *45*, 191–241; g) M. Arrowsmith, M. S. Hill in *Comprehensive Inorganic Chemistry II, Alkaline Earth Chemistry: Applications in Catalysis*, Vol. 1 (Eds.: J. Reedijk, K. Poeppelemeier), 1189–1216, Elsevier, Waltham, **2013**; h) S. Harder, *Chem. Rev.* **2010**, *110*, 3852–3876; i) A. G. M. Barrett, M. R. Crimmin, M. S. Hill, P. A. Procopiou, *Proc. R. Soc. London Ser. A* **2010**, *466*, 927–963.
- [11] a) C. Weetman, M. D. Anker, M. Arrowsmith, M. S. Hill, G. Kociok-Köhn, D. J. Liptrot, M. F. Mahon, *Chem. Sci.* **2016**, *7*, 628; b) C. Weetman, M. S. Hill, M. F. Mahon, *Chem. Commun.* **2015**, *51*, 14477–14480; c) M. D. Anker, M. S. Hill, J. P. Lowe, M. F. Mahon, *Angew. Chem. Int. Ed.* **2015**, *54*, 10009–10011; *Angew. Chem.* **2015**, *127*, 10147–10149; d) M. Arrowsmith, M. S. Hill, G. Kociok-Köhn, *Chem. Eur. J.* **2013**, *19*, 2776–2783; e) M. Arrowsmith, T. J. Hadlington, M. S. Hill, G. Kociok-Köhn, *Chem. Commun.* **2012**, *48*, 4567–4569; f) S. J. Bonyhady, S. P. Green, C. Jones,

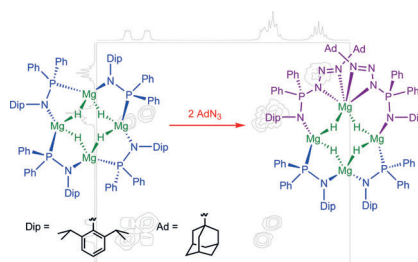
- S. Nembenna, A. Stasch, *Angew. Chem. Int. Ed.* **2009**, *48*, 2973–2977; *Angew. Chem.* **2009**, *121*, 3017–3021.
- [12] a) C. Weetman, M. S. Hill, M. F. Mahon, *Polyhedron* **2016**, *103*, 115–120; b) J. Intemann, M. Lutz, S. Harder, *Organometallics* **2014**, *33*, 5722–5729; c) M. Arrowsmith, M. S. Hill, T. Hadlington, G. Kociok-Köhn, C. Weetman, *Organometallics* **2011**, *30*, 5556–5559; d) M. S. Hill, G. Kociok-Köhn, D. J. MacDougall, M. F. Mahon, C. Weetman, *Dalton Trans.* **2011**, *40*, 12500–12509; e) M. S. Hill, D. J. MacDougall, M. F. Mahon, *Dalton Trans.* **2010**, *39*, 11129–11131.
- [13] a) J. Intemann, H. Bauer, J. Pahl, L. Maron, S. Harder, *Chem. Eur. J.* **2015**, *21*, 11452–11461; b) S. Harder, J. Spielmann, *J. Organomet. Chem.* **2012**, *698*, 7–14; c) J. Spielmann, F. Buch, S. Harder, *Angew. Chem. Int. Ed.* **2008**, *47*, 9434–9438; *Angew. Chem.* **2008**, *120*, 9576–9580; d) J. Spielmann, S. Harder, *Eur. J. Inorg. Chem.* **2008**, 1480–1486; e) J. Spielmann, S. Harder, *Chem. Eur. J.* **2007**, *13*, 8928–8938.
- [14] a) A. Stasch, *Dalton Trans.* **2014**, *43*, 7078–7086; b) A. Stasch, *Angew. Chem. Int. Ed.* **2012**, *51*, 1930–1933; *Angew. Chem.* **2012**, *124*, 1966–1969.
- [15] For reviews, see: a) Z. Fei, P. Dyson, *Coord. Chem. Rev.* **2005**, *249*, 2056–2074; b) M. Alajarin, C. López-Leonardo, P. Llamas-Lorente, *Top. Curr. Chem.* **2005**, *250*, 77–106.
- [16] a) A. Stasch, *Chem. Commun.* **2015**, *51*, 5056–5058; b) A. Stasch, *Angew. Chem. Int. Ed.* **2014**, *53*, 1338–1341; *Angew. Chem.* **2014**, *126*, 1362–1365.
- [17] A. R. Kennedy, R. E. Mulvey, S. D. Robertson, *Dalton Trans.* **2010**, *39*, 9091–9099.
- [18] For related phosphinoaminosilanes, see: a) T. Böttcher, C. Jones, *Dalton Trans.* **2015**, *44*, 14842–14853; b) J. Li, Y. Li, I. Purushothaman, S. De, B. Li, H. Zhu, P. Parameswaran, Q. Ye, W. Liu, *Organometallics* **2015**, *34*, 4209–4217; c) J. Wang, R. Liu, W. Ruan, Y. Li, K. C. Mondal, H. W. Roesky, H. Zhu, *Organometallics* **2014**, *33*, 2696–2703.
- [19] M. W. P. Bebbington, D. Bourissou, *Coord. Chem. Rev.* **2009**, *253*, 1248–1261.
- [20] A. L. Hawley, A. Stasch, *Eur. J. Inorg. Chem.* **2015**, 258–270.
- [21] For Mg-catalysed hydroborations of esters, see: D. Mukherjee, A. Ellern, A. D. Sadow, *Chem. Sci.* **2014**, *5*, 959–964.
- [22] a) H. Braunschweig, F. Guethlein, L. Mailänder, T. B. Marder, *Chem. Eur. J.* **2013**, *19*, 14831–14835; b) T. P. Onak, H. Landesman, R. E. Williams, I. Shapiro, *J. Chem. Phys.* **1959**, *63*, 1533–1535.
- [23] B. Marciniak, *Hydrosilylation: a comprehensive review on recent advances*, Springer, Berlin, **2009**.
- [24] N. L. Lampland, A. Pindwal, S. R. Neal, S. Schlauderer, A. Ellern, A. D. Sadow, *Chem. Sci.* **2015**, *6*, 6901–6907.
- [25] A.-K. Wiegand, A. Rit, J. Okuda, *Coord. Chem. Rev.* **2016**, *314*, 71–82.
- [26] For selected recent examples, see: a) W. Sattler, S. Rucolo, M. R. Chaijan, T. N. Allah, G. Parkin, *Organometallics* **2015**, *34*, 4717–4731; b) Z. Mou, H. Xie, M. Wang, N. Liu, C. Yao, L. Li, J. Liu, S. Li, D. Cui, *Organometallics* **2015**, *34*, 3944–3949; c) A. Rit, A. Zanardi, T. P. Spaniol, L. Maron, J. Okuda, *Angew. Chem. Int. Ed.* **2014**, *53*, 13273–13277; *Angew. Chem.* **2014**, *126*, 13489–13493; d) P. A. Lummis, M. R. Momeni, M. W. Lui, R. McDonald, M. J. Ferguson, M. Miskolzie, A. Brown, E. Rivard, *Angew. Chem. Int. Ed.* **2014**, *53*, 9347–9351; *Angew. Chem.* **2014**, *126*, 9501–9505; e) C. Boone, I. Korobkov, G. I. Nikonov, *ACS Catal.* **2013**, *3*, 2336–2340.

Received: April 7, 2016

Published online on ■ ■ ■, 0000

## FULL PAPER

**Forger of the rings:** Phosphinoamide ligands stabilise robust heteroleptic magnesium hydride complexes with unique structures. They are good hydromagnesian reagents and rapidly catalyse the hydroboration and hydrosilylation of ketones.



### Magnesium Complexes

*L. Fohlmeister, A. Stasch\**



**Ring-Shaped Phosphinoamido-Magnesium-Hydride Complexes: Syntheses, Structures, Reactivity, and Catalysis**

